Improved Surface Volume Estimates for Surface Irrigation Volume-Balance Calculations

E. Bautista, A.M.ASCE[1]; T. S. Strelkoff, M.ASCE[2]; and A. J. Clemmens, M.ASCE[3]

Abstract: This article reviews procedures for estimating surface storage in surface irrigation volume balance calculations. Those procedures are based on the assumption of a power law relationship for flow depth as a function of distance along the stream. The analysis uses zero-inertia simulation and a system of dimensionless variables to examine how the depth profile varies as a function of hydraulic conditions when infiltration is given by the empirical extended Kostiakov equation. Alternatives for approximating the exponent of the depth profile power law (β) are suggested. The magnitude of the resulting errors relative to zero-inertia model predictions is quantified. Results show that the range of variation for the parameter β increases with field slope, with increasing advance length relative to the maximum advance distance, and when infiltration rates are relatively constant with time during the irrigation event. Estimating β as a function of advance distance is most challenging under these conditions. Potentially large errors in the determination of β do not undermine the proposed procedures when the surface volume represents only a small fraction of the applied volume. Users of volume balance procedures need to be aware of conditions in which uncertain surface volume calculations can lead to potentially large volume balance errors and, thus, in which results need to be interpreted carefully. **DOI: 10.1061/(ASCE)IR.1943-4774.0000461.**

CE Database subject headings: Surface irrigation; Hydraulic models; Estimation; Water surface profiles; Analytical techniques.

Author keywords: Surface irrigation; Hydraulic models; Estimation; Water surface profiles; Analytical techniques.

Introduction

Volume balance calculations used in surface irrigation analyses estimate surface storage V_y at a given time t [T] as follows:

$$V_y(t) = \sigma_y \cdot A_0(t) \cdot x_A(t) \tag{1}$$

In Eq. (1), $A_0[L^2]$ = upstream flow area; σ_y [dimensionless] = shape factor that relates the average flow area to A_0; and $x_A[L]$ = distance advanced by the stream. The equation applies to the advance phase of the irrigation and to the runoff phase in open-end systems. Typical applications of Eq. (1) assume normal depth to compute A_0 and a constant σ_y, typically a value in the range 0.7–0.8. Those assumptions can lead to substantial errors because both the upstream depth y_0 and σ_y are functions of the unsteady flow. The volume balance model and its limitations is discussed in Strelkoff and Clemmens (2007).

Valiantzas (1993) proposed the following expression for evaluating y_0 (and, thus, A_0) in border irrigation

$$-\beta\frac{y_0}{x_A} = S_0 - \frac{q_0^2\, n^2}{c_u^2\, y_0^{10/3}} \tag{2}$$

Eq. (2) was derived by combining the following equations and evaluating the resulting expression at $x = 0$

$$\frac{\partial y}{\partial x} = S_f - S_0 \tag{3}$$

$$y(x) = y_0(1 - x/x_A)^\beta \tag{4}$$

$$S_f = \frac{q_0^2 n^2}{y^{10/3} c_u^2} \tag{5}$$

Eq. (3) is the zero-inertia equation (Strelkoff and Clemmens 2007), which is a statement of balance between the pressure gradient force (represented by the depth gradient $\partial y/\partial x$), the weight component of the fluid acting in the direction of flow (represented by the field bottom slope $S_0[L/L]$), and the friction force (represented by the friction slope $S_f[L/L]$). Eq. (4) is an empirical power relationship for flow depth $y[L]$ as a function of distance $x[L]$ along the stream. Eq. (5) is the Manning hydraulic resistance equation (for a channel of unit width). Other variables are y_0 = upstream flow depth [L]; β = power law exponent [-]; q_0 = inflow rate per unit width $[L^3/L]$; n = Manning roughness coefficient $[L^{1/6}]$; and c_u = units coefficient, 1.0 in the metric system and 1.486 in the English system. For $S_0 > 0$, Eq. (2) approximates the normal depth with increasing x_A.

Valiantzas (1993) also recognized that integration of Eq. (4) as a function of distance leads to an expression for V_y and, hence, for $\sigma_y(x_A)$. Therefore, for borders and basins

$$V_Y = W\int_{x=0}^{x=x_A} y_0(1 - x/x_A)^\beta dx = W\left(\frac{1}{\beta+1}\right) y_0 x_A \tag{6}$$

where $W[L]$ = basin width and other variables have been previously defined. Because $Wy_0 = A_0$, it follows that

[1]Research Hydraulic Engineer, USDA-ARS U.S. Arid Land Agricultural Research Center, 21881 North Cardon Lane, Maricopa AZ 85238 (corresponding author). E-mail: Eduardo.Bautista@ars.usda.gov

[2]Research Hydraulic Engineer, USDA-ARS U.S. Arid Land Agricultural Research Center, 21881 North Cardon Lane, Maricopa AZ 85238. E-mail: Theodor.Strelkoff@ars.usda.gov

[3]Senior Hydraulic Engineer, West Consultants, 8950 S 52nd Street Suite 210, Tempe, AZ 85284-1043; formerly, Laboratory Director, USDA-ARS Arid Land Agricultural Research Center. E-mail: bclemmens@westconsultants.com

Note. This manuscript was submitted on March 8, 2011; approved on February 7, 2012; published online on February 9, 2012. Discussion period open until January 1, 2013; separate discussions must be submitted for individual papers. This paper is part of the ***Journal of Irrigation and Drainage Engineering***, Vol. 138, No. 8, August 1, 2012. ©ASCE, ISSN 0733-9437/2012/8-715–726/$25.00.

$$\sigma_y = \frac{1}{\beta + 1} \tag{7}$$

When dealing with furrow irrigation systems, Eq. (2) is expressed as follows:

$$-\beta \frac{y_0}{x_A} = S_0 - \frac{Q_0^2 n^2}{c_u^2 A_0^2 R_0^{4/3}} \tag{8}$$

where R_0 = upstream hydraulic radius [L] and other variables are as previously defined.

The geometry of a furrow cross-section can be described by a parabola or a trapezoid. A parabolic geometry can be defined with the power law

$$T = cy^m, \quad A = \int_0^y T ds = \frac{c}{m+1} y^{m+1} \tag{9}$$

where T = top width; and c [L/L^m] and m [dimensionless] = empirical parameters. Combining Eqs. (4) and (9) and integration over the stream length yields

$$V_Y = \left(\frac{1}{\beta(m+1)+1}\right)\left(\frac{c}{m+1} y_0^{m+1}\right) x_A = \sigma_y A_0 x_A \tag{10}$$

This result was previously presented by Scaloppi et al (1995). The corresponding equations for a symmetrical trapezoidal furrow cross-section with side slope SS and bottom width BW are

$$A = y(BW + ySS) \tag{11}$$

$$V_Y = x_A \left(\frac{y_0 BW}{\beta + 1} + \frac{y_0^2 SS}{2\beta + 1}\right) \tag{12}$$

and

$$\sigma_y = \frac{1}{A_0}\left(\frac{y_0 BW}{\beta + 1} + \frac{y_0^2 SS}{2\beta + 1}\right) \tag{13}$$

Gillies and Smith (2005) applied Eq. (4) to the postadvance phase (prior to cutoff) in open-end systems by assuming that advance extends beyond the end of the field. A power advance law can be used to extrapolate the advance distance, but only for a limited time. The extrapolated advance distance, x_{PA}, substitutes x_A in Eq. (4) and, thus, in in the relationships for y_0 and σ_y. However, shape factors for the postadvance phase are calculated by integrating Eq. (6) or its furrow counterparts between $x = 0$ and L_f, the field length. The result for borders is

$$\sigma_y = \frac{1}{\beta + 1} \frac{x_{PA}}{L_f} \left[1 - \left(1 - \frac{L_f}{x_{PA}}\right)^{\beta+1}\right] \tag{14}$$

The corresponding expressions for parabolic and trapezoidal furrows are, respectively

$$\sigma_y = \frac{1}{\beta(m+1)+1} \frac{x_{PA}}{L_f} \left[1 - \left(1 - \frac{L_f}{x_{PA}}\right)^{\beta(m+1)+1}\right] \tag{15}$$

$$\sigma_y = \frac{x_{PA}}{A_0 L_f}\left\{\frac{y_0 BW}{\beta + 1}\left[1 - \left(1 - \frac{L_f}{x_{PA}}\right)^{\beta+1}\right] + \frac{y_0^2 SS}{2\beta + 1}\left[1 - \left(1 - \frac{L_f}{x_{PA}}\right)^{2\beta+1}\right]\right\} \tag{16}$$

Eq. (15) was previously presented by Gillies and Smith (2005).

The practical difficulty in using the previously discussed relationships is that β is a function of system properties and evolves with time and advance distance. Valiantzas (1993) proposed the following relationship for β:

$$\beta = \frac{0.45}{(1 + P)^{0.2}} \tag{17}$$

Eq. (17) was developed from graphical results presented in Katopodes and Strelkoff (1977), who examined the variation of y_0 and σ_y in border irrigation systems using the zero-inertia simulation model. These authors expressed the evolution of y_0 and σ_y with advance distance as a function of two dimensionless parameters, the exponent a [-] of the empirical Kostiakov infiltration equation

$$z = k\tau^a \tag{18}$$

and P [-], given by

$$P = \frac{q_0 S_0 (y_n/k)^{1/a}}{y_n^2} \tag{19}$$

In these expressions, z = infiltrated volume per unit area [L]; k = empirical infiltration constant [L/T^a]; and τ = infiltration opportunity time [T]. Katopodes and Strelkoff (1977) presented a series of curves for σ_y as a function of dimensionless advance distance for a single value of a (0.5). Those curves suggest that σ_y is relatively constant for small values of P, but variable when P is large. Nevertheless, Valiantzas (1993) derived Eq. (17) from the average value of each curve presented in Katopodes and Strelkoff (1977). Hence, it is important to emphasize that Eq. (17) is based only on border irrigation results, with infiltration given by the Kostiakov equation (and with $a = 0.5$) and that it assumes a constant exponent β for a given value of P.

The surface irrigation software WinSRFR (Bautista et al. 2009) uses Eqs. (2) and (8) for the calculation of y_0 in parameter estimation, design, and operational analysis. The program currently requires user-provided estimates for σ_y. A constant $\beta = 0.45$ was adopted in WinSRFR for the calculation of y_0. This choice was made on the basis of results presented by Bautista et al. (2008), who applied different constant values of β to calculate the upstream depth y_0 and then determined the relative error in comparison with y_0 values computed with the zero-inertia simulation model. The analysis was limited to border irrigation with infiltration given by the Kostiakov equation and did not examine the impact of this recommendation on the value of σ_y and, ultimately, V_y. Recommendations provided in previous studies for β (Valiantzas 1993; Scaloppi et al. 1995, Gillies and Smith 2005) are not based either on an analysis of the resulting volume balance errors.

Valiantzas (1997) and Monserrat and Barragan (1998) examined the variation of σ_y (and, thus, indirectly of β), but similar to previous studies, their results are based on the Kostiakov infiltration equation. Valiantzas (1997) proposed relationships for σ_y, but because his analysis was based on the kinematic wave model, those relationships can be applied only when the flow is kinematic.

The objectives of this study are, first, to examine the behavior of the exponent β in Eq. (4) as a function of hydraulic conditions. In contrast with previous studies, the analysis assumes that infiltration is given by the extended Kostiakov equation

$$z = k\tau^a + b\tau \tag{20}$$

The study also aims to develop an understanding of system factors that most influence the behavior of this parameter and to suggest values for use in routine surface volume calculations. Lastly, the study examines the volume balance errors that can result from using reasonable estimates of β. The analysis deals mostly with furrow irrigation, but limited results are presented for border irrigation.

Methodology

Similar to Katopodes and Strelkoff (1977), Valiantzas (1997), and Monserrat and Barragan (1998), this analysis uses a dimensionless formulation of the irrigation problem. This approach reduces the number of governing parameters and facilitates generalizing and displaying the results. A brief explanation of systems of dimensionless variables follows

In the governing equations of surface irrigation, the dependent surface-flow variables, Q and y, are functions of x and t, of parameters that describe the field geometry, hydraulic resistance, and infiltration characteristics, and of the boundary conditions (inflow rate). Nondimensional expressions for the variables and parameters (represented with the superscript *) are obtained by dividing the dimensional expressions by an appropriate reference variable (represented by the subscript R), a nonzero constant with the same dimensions.

$$x^* = \frac{x}{X_R}, \quad t^* = \frac{t}{T_R}, \quad Q^* = \frac{Q}{Q_R}, \quad y^* = \frac{y}{Y_R}, \quad A^* = \frac{A}{A_R}, \quad \tau^* = \frac{\tau}{T_R}, \quad z^* = \frac{z}{Y_R}; \quad S_0^* = \frac{S_0}{S_{0R}} \tag{21}$$

Different dimensionless systems can be derived depending on the type of irrigation system (graded furrow, graded border, level basin) and the choice of reference variables (Strelkoff and Clemmens 1994). This analysis uses the reference system proposed by Strelkoff (1985) for graded furrows

$$Q_R = Q_0; \quad Y_R = y_N(Q_0); \quad X_R = \frac{Y_R}{S_{0R}}; \quad T_R = \frac{X_R Y_R^2}{Q_R} \tag{22}$$

In these expressions, Q_0 = average unit inflow rate $[L^3/T]$; y_N = normal depth (calculated with the Manning equation, based on the reference slope) for the given Q_0; and S_{0R} = reference bottom slope, for convenience equal to the average slope. With these definitions and with n_R, a reference Manning n, dimensionless Q^*, n^*, and S_0^* are all equal to unity. Assuming negligible wetted perimeter effects on infiltration, infiltration volume per unit length (Z) is the product of the furrow spacing (W) and the infiltration volume per unit length and per unit furrow spacing (z)

$$Z = Wz = W(k\tau^a + b\tau) \tag{23}$$

It follows from Eqs. (21)–(23) that dimensionless advance as a function of dimensionless time is a function of four dimensionless parameters

$$x_A(t^*) = f(K^*, a, B^*, D_0^*) \tag{24}$$

Expressions for the dimensionless parameters are

$$K^* = \frac{WkT_R^a}{Y_R^2}; \quad B^* = \frac{WbT_R}{Y_R^2}; \quad D_0^* = \frac{A(Y_R)}{Y_R^2}\left[\frac{R(Y_R)}{Y_R}\right]\frac{n_R}{n}2/3 \tag{25}$$

In Eq. (25), D_0^* = parameter related to the channel conveyance and, therefore, a function of the cross-sectional geometry, the reference depth Y_R, and the dimensionless roughness characteristics, n/n_R.

A difficulty with using dimensionless formulations is that arbitrary dimensionless parameter combinations may not represent realistic physical systems. To avoid this problem and facilitate the interpretation of results, a limited set of scenarios was developed on the basis of a realistic range of physical conditions.

A basic set of 16 dimensionless scenarios was defined in terms of combinations of four slopes and four infiltration conditions, as given in Table 1. The table provides an identifier for each scenario, which are used subsequently in this article to label graphical results. The smallest slope value used in the analysis (0.00001) is smaller than the accuracy of practical land leveling operations and, thus, as nearly represents the case of zero-slope (because the dimensionless formulation employed in this paper uses normal depth for Y_R, it cannot be applied to cases with zero-slope). Infiltration conditions were defined on the basis of the time t_{req} needed to infiltrate a prescribed application depth z_{req}. An additional constraint on the infiltration parameters values was imposed by defining the infiltration parameter b as follows

$$b = \lambda\frac{z_{req}}{t_{req}} \tag{26}$$

In this expression, λ = parameter that determines the relative contribution of b to the infiltrated depth at t_{req}. When $\lambda = 0$, Eq. (20) reduces to the Kostiakov equation, whereas $\lambda = 1$ implies a constant infiltration rate throughout the irrigation event.

All scenarios were generated with $z_{req} = 0.1$ m, $W = 1$ m, SS = 1.5, $n = 0.04$. The initial set was developed for $a = 0.5$ and $\lambda = 0.4$ (i.e., 40% of the infiltration is contributed by the steady infiltration rate). Thus, for each t_{req} in Table 1 (2, 4, 8, and 16 h), the corresponding b values are 20, 10, 5, and 2.5 mm/h (Table 2). Given these inputs, the inflow for each scenario was calculated as follows. A spreadsheet was constructed containing all the needed dimensional inputs (S_0, z_{req}, t_{req}, λ, W, SS, and n) for all 16 scenarios, the infiltration relationships [Eqs. (23) and (26)], and the dimensionless relationships [Eqs. (22) and (25)]. Reasonable initial values for Q and BW were assumed for scenario 1 (4 l/s and 0.2 m,

Table 1. Identifiers for the 16 Furrow Irrigation Scenarios

	S_0			
t_{req} (h)	0.00001	0.0001	0.001	0.01
2	1	5	9	13
4	2	6	10	14
8	3	7	11	15
16	4	8	12	16

Table 2. Dimensionless Parameters for the Furrow Irrigation Scenarios: $\lambda = 0.4$; $a = 0.5$

		S_0			
		0.00001	0.0001	0.001	0.01
		($K^* = 6.5$; $D_0^* = 2.1$)	($K^* = 2.7$; $D_0^* = 3.65$)	($K^* = 1.14$; $D_0^* = 8.0$)	($K^* = 0.05$; $D_0^* = 22.5$)
t_{req} (h)	b(mm/h)	B^*			
2	20	3.88E+01	2.28E+00	1.28E-01	6.90E-03
4	10	2.65E+01	1.56E+00	8.70E-02	4.70E-03
8	5	1.81E+01	1.06E+00	6.00E-02	3.30E-03
16	2.5	1.25E+01	7.38E-01	4.10E-02	2.20E-03
		$L*$			
2	20	1.29E-02	2.19E-01	3.91E+00	7.22E+01
4	10	1.88E-02	3.20E-01	5.71E+00	1.05E+02
8	5	2.75E-02	4.67E-01	8.34E+00	1.54E+02
16	2.5	4.01E-02	6.82E-01	1.22E+01	2.24E+02

respectively). This selection yielded a value close to 6.5 for K^* and 2.1 for D_0^*. The values of K^* and D_0^* were then rounded to 6.5 and 2.1, respectively, by adjusting Q and BW. Starting from the same initial guesses as for scenario 1, Q and BW were adjusted for scenarios 2–4 (with the same slope) to force $K^* = 6.5$ and $D_0^* = 2.1$. The values of Q and BW obtained for scenario 1 were copied to scenario 5, representing the same t_{req} conditions. Adjustments were then made to Q and BW in scenarios 5–8 to force K^* and D_0^* to the same constant values (2.7 and 3.65, Table 2). This set of computations was repeated for scenarios 9–12, and 13–16. The resulting Q and BW are provided in Table 3. Because increasing t_{req} values imply decreasing infiltration rates, B^* decreases as t_{req} increases for any K^*.

For each scenario, the dimensionless furrow length L_f^* (Table 2) was determined as $L_f^* = \lambda(1/B^*)$. The corresponding dimensional lengths L_f (Table 3) were then determined as $L_f = L_f^* X_R$. In the first calculation, the ratio $1/B^*$ is the maximum advance distance, i.e., the advance distance at which the inflow rate matches the steady infiltration rate over the wetted length of the furrow. In dimensional terms, this maximum distance is given by the ratio Q_0/bW. The approach used to determine L_f^*, expressed as a function of λ (the relative contribution of the steady infiltration rate), results in realistic infiltration depths (relative to the infiltration target z_{req}) when inflow is cut off at the final advance time (Table 3). As an aside, the advance problem becomes poorly posed (predictions are very sensitive to small changes in inputs) when the wetted furrow length approximates $1/B^*$. Hence, this maximum distance cannot be attained either in practice or computationally (except in the theoretical case $\lambda = 1.0$).

Four additional sets of scenarios were examined. Two of those sets were generated with $a = 0.5$, but with $\lambda = 1.0$ and $\lambda = 0.1$. The corresponding dimensionless parameters are given in Tables 4 and 5, respectively. Because the values of the infiltration exponent a and D_0^* were not modified with respect to the first set of scenarios, and the dimensionless field lengths were defined again as $L_f^* = \lambda \cdot (1/B^*)$, these new scenarios represent the same combinations of dimensional input variables as before (Table 3) except for the values of b and k. Irrigated soils typically exhibit a declining infiltration rate; nevertheless, scenarios with $\lambda = 1.0$ were included to illustrate the maximum range for β. The last two sets were developed with $\lambda = 0.4$, but with $a = 0.3$ and 0.7. These changes have no effect on B^*, D_0^*, and L_f^* (Table 2) and the corresponding dimensional variables, but they affect K^*, which is no longer constant for scenarios with the same slope (Table 6). For this new set of scenarios, cutoff at the final advance time produces final infiltration depths that are only slightly different from those given in Table 3 (not shown).

Each scenario was simulated with the zero-inertia engine of the WinSRFR program (Bautista et al. 2009). WinSRFR calculates σ_y at each time step [using Eq. (1)]. These values were entered into Eq. (13) to solve for β.

Relationships among dimensionless variables, and between dimensionless and dimensioned variables, merit further discussion. First, in the dimensionless formulation employed in this paper, K^* and B^* are independent governing parameters. In the proposed scenarios, these parameters are linked through t_{req}, a, and λ. Hydraulically related scenarios, but with substantially different values of K^* and B^*, can be created for a given t_{req} by altering the values of λ and/or a (Tables 4–6). Second, with these scenarios, the order of magnitude of B^* is largely determined by the field slope. Consider for example, scenarios 1 ($S_0 = 0.00001$, $B^* = 3.88E+01$) and 13 ($S_0 = 0.01$, $B^* = 6.90E-03$) in Table 2. B^* differs by four orders of magnitude. Dimensioned scenarios with $S_0 = 0.00001$ and $B^* = 6.90E-03$ can be generated, but that would require a near-zero value of b (hence, a different infiltration

Table 3. Discharge, Bottom, Width, and Furrow Length for the Furrow Irrigation Scenarios

	S_0			
	0.00001	0.0001	0.001	0.01
t_{req} (h)	$Q(l/s)$			
2	4.12	4.09	4.09	4.00
4	2.49	2.48	2.47	2.42
8	1.51	1.50	1.49	1.46
16	0.91	0.90	0.90	0.88
	BW(m)			
2	0.215	0.215	0.216	0.216
4	0.18	0.180	0.179	0.179
8	0.150	0.150	0.148	0.148
16	0.120	0.120	0.122	0.122
	$L_f(m)$			
2	296.5	294.3	294.5	288.4
4	358.3	355.7	355.9	348.3
8	432.9	429.6	430.0	420.8
16	522.8	518.9	519.1	508.3
	Average infiltrated depth (mm)			
2	111	106	86	66
4	97	92	76	61
8	86	81	68	57
16	78	73	62	55

Table 4. Dimensionless Parameters for the Furrow Irrigation Scenarios: $\lambda = 1.0$; $a = 0.5$

		S_0			
		0.00001	0.0001	0.001	0.01
		($K^* = 0$; $D_0^* = 2.1$)	($K^* = 0$; $D_0^* = 3.65$)	($K^* = 0$; $D_0^* = 8.0$)	($K^* = 0$; $D_0^* = 22.5$)
t_{req} (h)	b(mm/h)	$B*$			
2	50	9.70E+01	5.70E+00	3.20E-01	1.73E-02
4	25	6.62E+01	3.89E+00	2.19E-01	1.19E-02
8	12.5	4.53E+01	2.66E+00	1.50E-01	8.13E-03
16	6.25	3.13E+01	1.84E+00	1.03E-01	5.57E-03

Table 5. Dimensionless Parameters for Furrow Irrigation Scenarios with $\lambda = 0.1$, $a = 0.5$

		S_0			
		0.00001	0.0001	0.001	0.01
		($K^* = 9.75$; $D_0^* = 2.1$)	($K^* = 4.05$; $D_0^* = 3.65$)	($K^* = 1.17$; $D_0^* = 8.0$)	($K^* = 0.75$; $D_0^* = 22.5$)
t_{req} (h)	b(mm/h)	$B*$			
2	5	9.70E+00	5.70E-01	3.20E-02	1.70E-03
4	2.5	6.62E+00	3.89E-01	2.19E-02	1.20E-03
8	1.25	4.53E+00	2.66E-01	1.50E-02	8.00E-04
16	0.625	3.13E+00	1.84E-01	1.03E-02	6.00E-04

Table 6. K^* for the Furrow Irrigation Scenarios: $\lambda = 0.4$; $a = 0.3$; and $a = 0.7$

S_0	0.00001	0.0001	0.001	0.01
t_{req} (h)	$K^*(a = 0.3)$			
2	2.71	2.46	2.33	2.36
4	3.15	2.86	2.71	2.74
8	3.66	3.32	3.15	3.19
16	4.26	3.87	3.66	3.71
	$K^*(a = 0.7)$			
2	15.61	2.97	0.559	0.1062
4	13.42	2.55	0.480	0.0913
8	11.54	2.19	0.413	0.0785
16	9.92	1.89	0.355	0.0675

behavior from the one assumed in this analysis). Lastly, a constant K^* imposes a relationship between t_{req} and Q for scenarios with a common slope. This relationship constrains the physical field lengths considered in the analysis and the resulting average infiltration depths to values close to z_{req} (Table 3).

Results

Variation of β with Advance Distance

Fig. 1 displays β as a function of x_A^*(in logarithmic scale) for each scenario. The curves are labeled according to the identifiers of Table 1. Because L_f^* is a function of $1/B^*$ and values of B^* generated for a given K^* are of a similar order of magnitude (Table 2), curves generated for the same K^* plot in the same x_A^* range.

Results illustrate the fundamental behavior of β. During early advance, flow rate differences along the stream are small. As a result, flow depth is rising rapidly everywhere and is relatively uniform except near the front of the stream, where it is changing rapidly. Because the profile is steepening, β decreases initially. As the stream elongates, cumulative infiltration losses cause increasing inflow rate differences and more gradual depth variations with distance. Hence, during later advance, β increases with x_A^*.

Relevant to the objectives of this study is the range of β. In Fig. 1, the range of β increases with decreasing K^* and to a lesser degree with decreasing B^*. However, as was noted before, a constant K^* imposes a relationship between infiltration and discharge for a given slope. Thus, results show that the range of β is strongly dependent on slope, at least for realistic combinations of dimensioned inputs. With mild slopes, a relatively large depth gradient is needed to drive the flow. Thus, β varies over a narrow range. β attains smaller values and varies over the widest range at short advance distances when the slope is steep because normal flow is attained rapidly and depth varies abruptly near the front of the wave.

Numerical limitations of these results need to be noted. The initial value of β depends on the spatial weighting factor used to discretize the governing flow equations. The influence of that initial value persists for a few time steps in the calculations. Development of the curves for $K^* = 0.5$ ($S_0 = 0.01$) present another numerical problem. When the field bottom slope is sufficiently steep, the flow is essentially kinematic and flow depth variation near the advancing front are also steep. The zero-inertia model cannot describe adequately these pronounced depth variations (a criterion that can be used to determine when the flow is kinematic is provided in Strelkoff and Clemmens 2007). As a result, the computed y_0, and thus β, oscillates at small x_A^*. A smooth relationship for $\beta(x_A^*)$, which is depicted in the figure, was generated by solving for σ_y with Eq. (1) but using the normal flow area A_n instead of the A_0 computed with the zero-inertia model. An alternative approach is to compute the flow with the kinematic wave model. However, that approach changes substantially the $\beta(x_A^*)$ relationship at small values of x_A^* because the kinematic wave model assumes a nonzero depth at the wave front. A nonzero depth at the tip is incompatible with Eq. (4), and thus, with Eqs. (2) and (8).

Effect of λ and a

The parameter λ determines the advance distance at which β will attain its final and maximum value, $x_{A\max} = 1/B^*$. Thus, β will vary over a wide range if a field is long relative to $1/B^*$, but over a narrow range in the opposite case. The $\beta(x_A^*)$ relationships depicted in Fig. 2 ($\lambda = 1.0$) Fig. 3 ($\lambda = 0.1$) illustrate primarily the effect of relative length. Again, the curves are numbered according to the identifiers of Table 1. The curves of Fig. 2 ($\lambda = 1.0$) show a much wider range than in Fig. 1, primarily because $L_f^* = 1/B^*$ with these scenarios. The curves of Fig. 3 exhibit a much narrower range because L_f^* is only a tenth of $1/B^*$. In these cases, β continues to increase with longer fields.

Although not as evident, λ affects also the minimum value of β. Advance will be faster and require less inflow volume for a given distance when the infiltration rate is relatively constant (i.e., when λ is large). Under those conditions, and with a large slope, a steep wave front will persist for longer advance distances. As was noted before, β cannot attain small values with mild slopes. Thus, the curves of Fig. 2 attain smaller minimum values than in Fig. 1, but the effect is noticeable only for scenarios 9–16. With a smaller

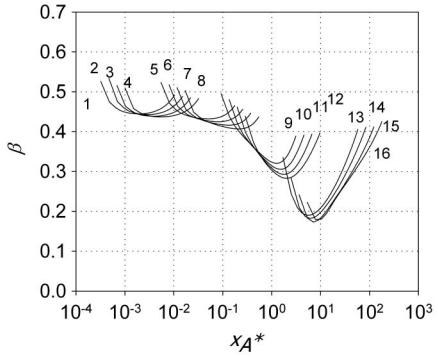

Fig. 1. β as a function of x_A^* for furrow irrigation scenarios with $\lambda = 0.4$, $a = 0.5$

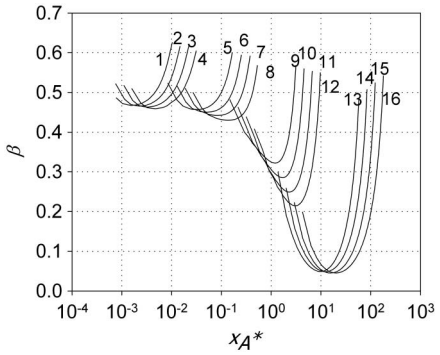

Fig. 2. β as a function of x_A^* for furrow irrigation scenarios with $\lambda = 1.0$, $a = 0.5$

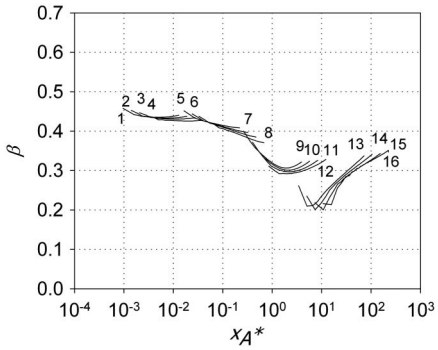

Fig. 3. β as a function of x_A^* for furrow irrigation scenarios with $\lambda = 0.1$, $a = 0.5$

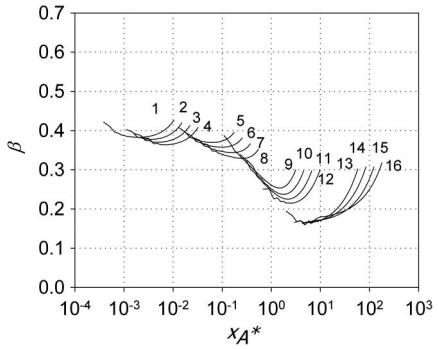

Fig. 4. β as a function of x_A^* for furrow irrigation scenarios with $\lambda = 0.4$, $a = 0.3$

λ (Fig. 3), the minimum value of β shifts upward, but the effect is minor.

Similar to the value of λ, infiltration rates become more constant with time as the exponent a increases (for times less than t_{req}.) As a result, and in comparison with the results computed with $a = 0.5$ (Fig. 1), the range of the $\beta(x_A^*)$ relationships narrows when $a = 0.3$ (Fig. 4) but widens when $a = 0.7$ (Fig. 5). However, the $\beta(x_A^*)$ relationships of Fig. 4 are shifted downward in comparison with those of Fig. 1 (and also of Fig. 3). Thus, a smaller exponent a produces steeper wave fronts for the advance distances considered in the analysis (likely because infiltration rates and flow rates are varying most rapidly near the front of the wave). In contrast, the $\beta(x_A^*)$ relationships of Fig. 5 ($a = 0.7$) are shifted upward (albeit slightly) with respect to those of Fig. 1, but only for mild slopes (scenarios 1–8).

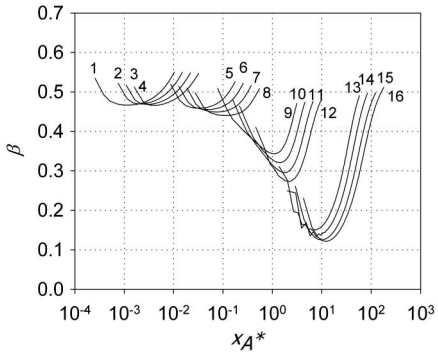

Fig. 5. β as a function of x_A^* for furrow irrigation scenarios with $\lambda = 0.4$, $a = 0.7$

The practical implication of these results is that a large variation in the value of β as a function of advance distance can be expected when infiltration rates are relatively constant with time and the field length is close to the theoretical maximum advance distance. Such conditions are more likely to be encountered in practice when λ is large and $a = 0.5$ or larger, i.e., with light soils. Characterizing $\beta(x_A^*)$ is most difficult under those conditions, especially if the slope is large. By the same token, β can be expected to be relatively constant when infiltration rates vary substantially during the course of the irrigation event, leading to a small contribution by the steady-state term. Such conditions occur when λ is small and $a = 0.5$ or less, which is typical of heavier soils. In those cases, β will vary over a narrow range even for long fields relative to the maximum advance distance, especially for mild slopes. If infiltration is assumed to follow the Kostiakov equation ($\lambda = 0$), then the range for β is unrelated to $1/B^*$ because advance is theoretically infinite. Independently of the fact that it reveals a relationship between β and $1/B^*$, the extended Kostiakov equation should be used for practical analyses of irrigation systems because it imposes limits on the maximum distance that water can advance down a field and should lead to more conservative design and operational recommendations.

Proposed β Relationships

An explicit relationship for β as a function of K^*, a, B^*, and x_A^* is desirable for routine volume balance calculations. Such a relationship cannot be defined easily from Figs. 1–5, and even if available, it would be of limited value when applying the volume balance method to parameter estimation problems (because K^*, a, and B^* are unknown). Of interests, then, is to suggest simple estimates of β that can be used for routine calculations.

Relationships for β as a function of S_0 alone are proposed, of the form

$$\beta(S_0) = b_0 + m \cdot \log_{10}(S_0) \tag{27}$$

Parameters for Eq. (27) were determined for each group of scenarios (Figs. 1–5) by determining a representative point for each curve and fitting from those points. The midpoint between the minimum and final β values was selected as that representative point. The implications of using an alternative representative point are discussed subsequently. Regression parameters for each group of scenarios, including the coefficient of determination r^2, are presented in Table 7.

Table 7. Regression Parameters and r^2 for the Proposed $\beta(S_0)$ Relationships [Eq. (27)] for Each Scenario Set, and Predicted Values of $\beta(S_0)$

	Scenario set				
	$\lambda = 0.4$ $a = 0.5$	$\lambda = 1.0$ $a = 0.5$	$\lambda = 0.1$ $a = 0.5$	$\lambda = 0.4$ $a = 0.3$	$\lambda = 0.4$ $a = 0.7$
Parameters	Regression values				
m	−0.0588	−0.0886	−0.0563	−0.0611	−0.0671
b_0	0.18	0.1281	0.1595	0.0984	0.1903
r^2	0.96	0.91	0.95	0.93	0.95
S_0	Predicted β				
0.00001	0.474	0.571	0.441	0.404	0.526
0.0001	0.415	0.483	0.385	0.343	0.459
0.001	0.356	0.394	0.328	0.282	0.392
0.01	0.298	0.305	0.272	0.221	0.325

y_0 and σ_y values derived with the $\beta(S_0)$ estimates will be, to a lesser or greater degree, inaccurate relative to the zero-inertia model. Differences will result, first, from the assumption of a constant β for any advance distance and, second, from the choice of $\beta(S_0)$ relationship, which may be inadequate for a given field. The subsequent paragraphs analyze the potential magnitude of the differences and the implications for volume balance analyses. The analysis is limited by the range of hydraulic characteristics examined in Figs. 1–5, but still should give us an idea of conditions under which reliable volume balance results can be generated with simple β estimates and conditions under which those estimates need to be refined.

For each group of scenarios, y_0, and σ_y were calculated as a function of x_A^* using, respectively, Eqs. (8) and (12). Initial calculations used the $\beta(S_0)$ relationship derived specifically for that set of scenarios, but additional calculations were carried out also with the relationship derived from a different set of scenarios. Those results were then used to determine the relative y_0 error (Ey_0), relative σ_y error ($E\sigma_y$), and the volume balance error (E_{VB}), which are defined as

$$E_{y_0} = (y_0^\beta - y_0^{ZI})/y_0^{ZI} \tag{28}$$

$$E_{\sigma y} = (\sigma_y^\beta - \sigma_y^{ZI})/\sigma_y^{ZI} \tag{29}$$

$$E_{VB} = (V_y^\beta - V_y^{ZI})/V_{app}^{ZI} \tag{30}$$

In these expressions, the superscript β refers to variables calculated with the volume balance procedures; the superscript ZI refers to variables simulated with the zero-inertia model; and V_{app} = applied volume (sum of the infiltrated and surface volume). In this discussion, error denotes systematic differences between volume balance and zero-inertia calculations and not necessarily the errors that may result in practical volume balance calculations, which ultimately depend on the ability to characterize pertinent system inputs.

Errors were computed for the scenarios of Fig. 1 using the $\beta(S_0)$ relationship specific to those scenarios (with the regression parameters of column $a = 0.4$, $\lambda = 0.4$ in Table 7). The errors (Ey_0—dashed line; $E\sigma_y$ —dash-dot line; and E_{VB}—solid line) are plotted in Fig. 6 as a function of a new dimensionless variable, the relative advance distance $x_A^*/x_{Amax}^* = x_A^* B^*$. Given that $L_f^* = \lambda \cdot (1/B^*)$, the maximum value of $x_A^* B^*$ for each plot is $\lambda = 0.4$.

Four things need to be noted about the results of Figure 6. First, Eq. (8) is sensitive to β when S_0 is small, but becomes increasingly insensitive as flow depth approaches its normal value, which is more likely with increasing slope and advance distance. Eq. (12) is unaffected by these variables. Thus, y_0 estimates derived with a rough estimate of β are more reliable than estimates of σ_y especially with large slopes and advance distances. Second, $|E_{VB}|$ can be

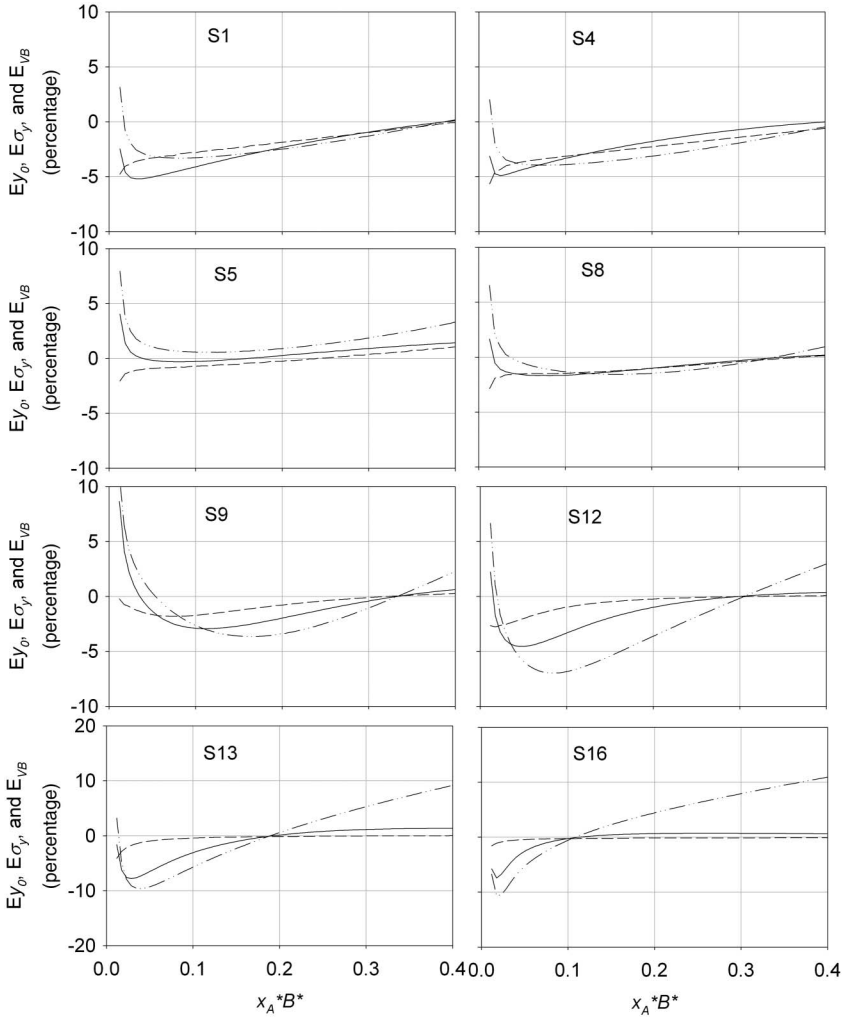

Fig. 6. Relative depth error Ey_0 (dashed line), relative shape factor error $E\sigma_y$ (dash-dot line), and volume balance error E_{VB} (solid line) for furrow irrigation scenarios with $\lambda = 0.4$, $a = 0.5$

very large at short advance distances, not only because both $|Ey_0|$ and $|E\sigma_y|$ are large, but also because surface storage is a large fraction of the applied volume. The impact is greatest with steep slopes, as shown by scenarios 13 and 16 in Fig. 6, for which $|E_{VB}|$ is nearly 10% when $x_A^* B^* < 0.1$. Third, although $|E\sigma_y|$ can be very large, its effect on $|E_{VB}|$ decreases with $x_A^* B^*$ because the surface volume grows slowly in comparison with the applied and infiltrated volumes as the advance slows down. This is particularly true with steep slopes, because flow depths are small. Lastly, the errors of Fig. 6 depend on the representative value used to derive the $\beta(S_0)$ relationship. If the final value of $\beta(x_A^*)$ curves (Fig. 1) had been chosen instead of the midpoint as the representative value, the error curves of Fig. 5 would shift downward, i.e., errors would be greater at smaller $x_A^* B^*$ and smaller near $x_A^* B^* = 0.4$. Choosing the minimum value of the $\beta(x_A^*)$ curves as the representative point would have the opposite effect and increase the errors for large $x_A^* B^*$. Overall, the midpoints seem like a reasonable choice, especially considering that the sensitivity of E_{VB} to β decreases with advance distance.

Fig. 7 presents the errors computed for the scenarios of Fig. 2. As with the previous figure, the $\beta(S_0)$ relationship developed from this set of scenarios was used in the calculations (parameters given in the column $\lambda = 1.0$, $a = 0.5$ in Table 7). As expected, the relative errors are greater than in Fig. 6 because of β varies over a larger range when $\lambda = 1.0$ than with $\lambda = 0.4$. In the figure, $|E_{VB}|$ exceeds 10% with mild slopes and 20% with steep slopes. More importantly, because the applied volume grows slowly relative to surface storage (i.e., the infiltration volume for a given advance distance is much less than for the scenarios of Fig. 6), the potential for a large E_{VB} does not decrease with advance distance. Accurate β estimates are always needed under these conditions.

Figs. 8–10 present the errors computed for the scenarios of Figs. 3–5. In each case, a first set of results (a) was calculated with the $\beta(S_0)$ relationship specific to that group of scenarios and a second (b) with the $\beta(S_0)$ relationship developed for $\lambda = 0.4$, $a = 0.5$. The graphs present E_{VB} alone and include only one scenario from each slope group (1, 6, 11, and 16).

In Fig. 8(a), $|E_{VB}|$ is less than 1% except at very short advance distances. Small errors were expected given the narrow range of $\beta(x_A^*)$ when $\lambda = 0.1$. Much larger errors were calculated for scenarios 1 and 6 when using the $\beta(S_0)$ relationship developed from ($\lambda = 0.4$, $a = 0.5$) [Fig. 8(b)]. These absolute errors are nearly an order of magnitude greater than in Fig. 8(a) (but still less than 5%). The choice of $\beta(S_0)$ relationship has little or no effect on the magnitude of the errors when the flow is near or fully kinematic (scenarios 11 and 16, respectively). The errors illustrated in Fig. 8(b) may be acceptable considering the uncertainty of other inputs required for the calculations; still, it should be clear that greater care

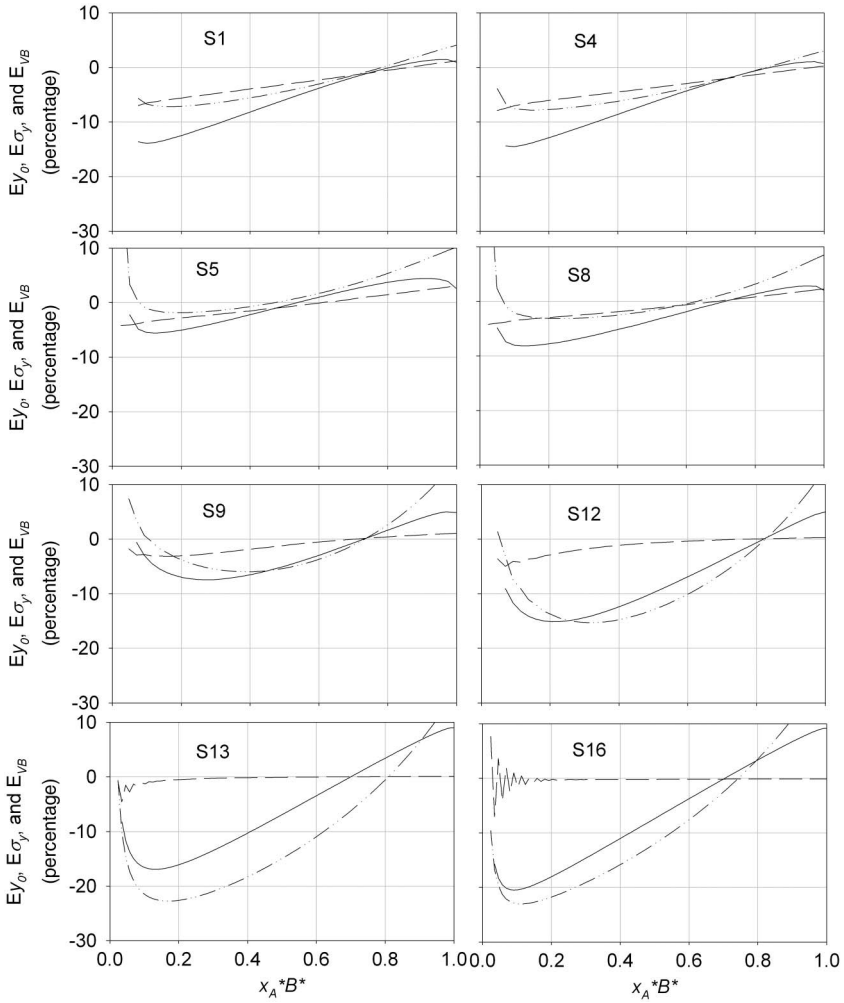

Fig. 7. Relative depth error Ey_0 (dashed line), relative shape factor error $E\sigma_y$ (dash-dot line), and volume balance error E_{VB} (solid line) for furrow irrigation scenarios with $\lambda = 1.0$, $a = 0.5$

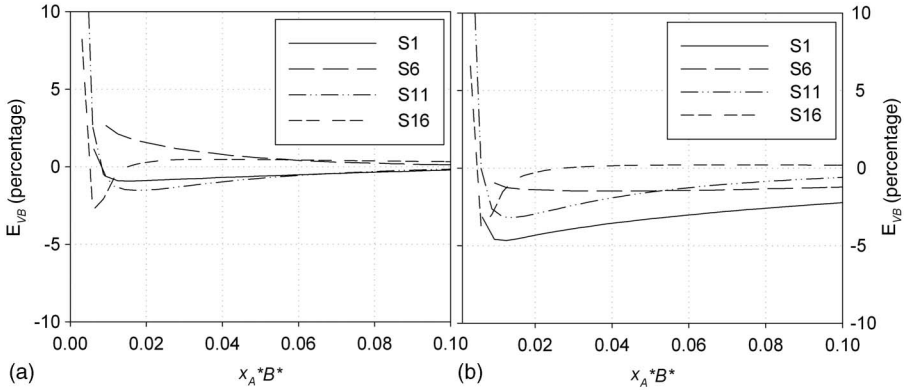

Fig. 8. Volume balance errors for furrow irrigation scenarios with $\lambda = 0.1$, $a = 0.5$

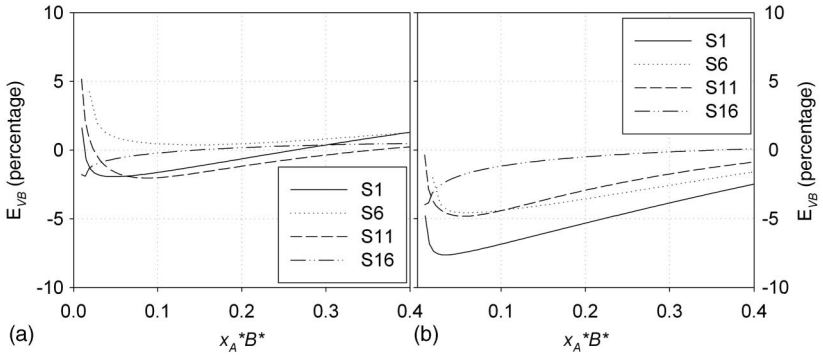

Fig. 9. Volume balance errors for furrow irrigation scenarios with $\lambda = 0.4$, $a = 0.3$

must be exercised when selecting a $\beta(S_0)$ relationship with small slopes.

Similar to the previous set of results, the absolute errors in Fig. 9(a) vary over a narrow range (less than 2% for most advance distances) when using β values specific to the scenarios presented in that figure ($\lambda = 0.4$, $a = 0.3$). In Fig. 9(b), so-called incorrect β estimates (derived assuming $\lambda = 0.4$, $a = 0.5$) lead to absolute errors that are nearly four times greater than in Fig. 9(a). Again, the potential for large errors increases with increasing slope and decreasing relative advance distances ($x_A^*B^* < 0.2$). Errors were also calculated for this group of scenarios using the $\beta(S_0)$ relationship of the previous example ($\lambda = 0.1$, $a = 0.5$). Those errors, which are not illustrated, were less than in Fig. 9(b). Thus, if the soil is heavy and/or the final infiltration rate is expected to be small for a particular analysis, β values should be derived from Figs. 3 and 4.

Fig. 10 depicts the errors computed for the scenarios of Fig. 5 ($\lambda = 0.4$, $a = 0.7$). Comparison of Figs. 10(a) and 10(b)– shows that the potential for large errors is substantial at small advance distances ($x_A^*B^* < 0.1$) and especially with a steep slope (scenario 16). Absolute errors [Fig. 10(a)] are as much as 15% when using $\beta(S_0)$ estimates derived from the scenarios with $\lambda = 0.4$, $a = 0.7$ and, in fact, improve slightly when using the $\beta(S_0)$ estimates derived from the scenarios with $\lambda = 0.4$, $a = 0.5$. For longer advance distances ($x_A^*B^* > 0.2$), E_{VB} values are generally less than 3%, even when using the $\beta(S_0)$ estimates derived from Fig. 1 [Fig. 10(b)]. Errors are much greater when using the $\beta(S_0)$ relationship derived from Fig. 4 (results not shown). In principle, the curves of Figs. 5 or 1 can be used with lighter soils, as those soils are associated with larger values of a and λ. However, the resulting V_y estimates cannot be expected to be reliable except for long advance distances.

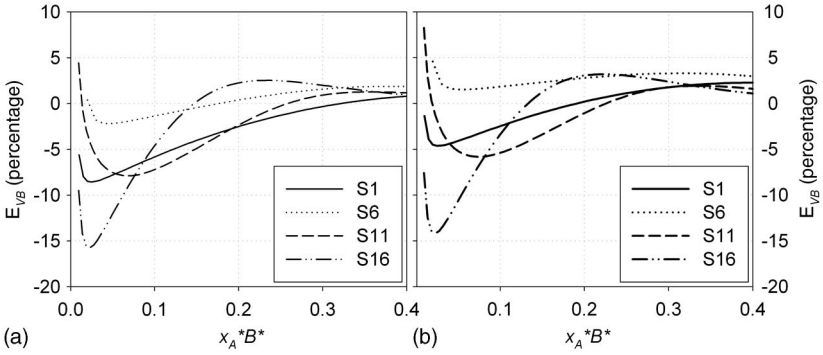

Fig. 10. Volume balance errors for furrow irrigation scenarios with $\lambda = 0.4$, $a = 0.7$

Relationships for Border Irrigation

$\beta(x_A^*)$ was examined for a limited number of border irrigation scenarios, with the goal of contrasting the relationships with the furrow cases. A dimensionless system of variables for borders (Strelkoff and Clemmens 1994), similar to the one described in this paper, was used to develop the border irrigation scenarios. For borders, advance is a function of three dimensionless variables, k^*, b^*, and the infiltration exponent a. Expressions for the parameters are provided in that reference. The dimensionless k^* and b^* used in this analysis are given Table 8. These parameter values were developed from dimensioned scenarios, using the same bottom slope and t_{req} combinations of Table 1, with $z_{req} = 100$ mm, $n = 0.2$, $a = 0.5$, and with the unit flow rates given in Table 9. Dimensionless length was calculated as $L_f^* = \lambda/b^*$, which with the given inputs translates into a dimensional value of $L_f = 360$ m for all of these scenarios.

The $\beta(x_A^*)$ relationships for borders (Fig. 11) are very similar to the ones developed for furrows (Fig. 1), despite the difference in cross-sectional geometry and the larger value of n used in this set of calculations. This suggests that $\beta(x_A^*)$ relationships for other furrow geometries and roughness values (i.e., other D_0^* values based on realistic combinations of dimensioned variables) are not very different from the ones presented in Figs. 1–5. Hence, the $\beta(S_0)$ relationships proposed in this paper should provide reasonable estimates for borders and other furrow configurations.

Practical Example

Perea (2005) reported four furrow irrigation evaluation data sets that include depth hydrograph measurements along the field. Those measurements can be used to determine surface volumes as a function of time. The data set identified in his dissertation as Furrow 1 was used for this example. Relevant data are the following: $L_f = 168.5$ m; $S_0 = 0.00018$; $Q_{avg} = 1.41$ l/s; cross-section = trapezoidal; $B_0 = 0.07$ m; and SS = 2.7. The data are available from the first author upon request. Surface volume as a function

Table 8. Dimensionless Parameters for the Border Irrigation Scenarios: $\lambda = 0.4$; $a = 0.5$

		S_0			
		0.00001	0.0001	0.001	0.01
		($K^* = 3.162$)	($K^* = 1.0$)	($K^* = 0.316$)	($K^* = 0.1$)
t_{req} (h)	b(mm/h)	B^*			
2	20	5.57E+01	2.79E+00	1.40E-01	7.01E-03
4	10	3.67E+01	1.84E+00	9.23E-02	4.63E-03
8	5	2.42E+01	1.21E+00	6.09E-02	3.05E-03
16	2.5	1.60E+01	8.01E-01	4.02E-02	2.01E-03

Table 9. Unit Flow Rates for the 16 Border Irrigation Scenarios: $\lambda = 0.4$; $a = 0.5$

	S_0			
	0.00001	0.0001	0.001	0.01
t_{req} (h)	Q(l/s/m)			
2	5.00	5.00	5.00	5.00
4	2.50	2.50	2.50	2.50
8	1.25	1.25	1.25	1.25
16	0.63	0.63	0.63	0.63

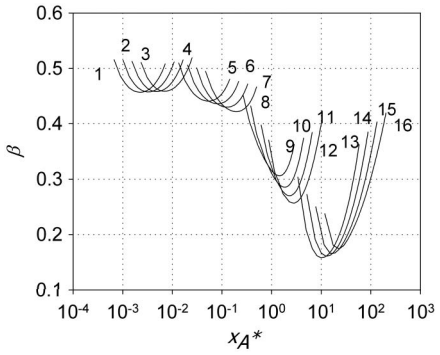

Fig. 11. β as a function of x_A^* for the border irrigation scenarios with $\lambda = 0.4$, $a = 0.5$

time and the Manning n were determined from the depth hydrographs using the procedures described in Strelkoff et al. (1999). Eq. (8) was used to estimate y_0, whereas Eqs. (12) and (16) were used to calculate σ_y during the advance phase and postadvance phases, respectively. A power law derived from the advance data was used to compute x_{PA} at selected postadvance times ($x_{PA} = pt^r$, with $p = 0.394$ m/ min^r, $r = 0.64$). The soil for the test is a sandy loam and exhibits a fairly large near-steady infiltration rate. Thus, Eq. (27) with the parameters derived from Fig. 1 was used to determine $\beta = 0.4$. Data and calculations are summarized in Table 10. With trapezoidal furrows, σ_y is a function of y_0. Thus, the computed σ_y varies with time even if β is constant. The estimated V_y tracked reasonably well the observed values for times less than 200 min. The last column in Table 10 presents the calculated volume balance errors, which are very reasonable during advance, but which increase during the postadvance phase. Clearly, the standard volume balance assumptions (upstream normal depth, $\sigma_y = 0.77$) would result in much larger differences than shown in the table. The loss of accuracy during the postadvance phase is explained by the extrapolation of advance distance. In the first author's experience, the Gillies and Smith (2005) procedure for predicting surface storage during the postadvance phase yields reasonable results when the inflow rate is constant and the advance trajectory is extrapolated for less than twice the final advance time. For longer times, advance rate can be expected to decline sharply and, thus, x_{PA} should be assumed to remain constant. The extrapolation is particularly inadequate for this problem because the inflow rate delivered to the field declined after the water reached the end of the field.

Discussion

The proposed relationships of Figs. 1–5 can be used to derive β estimates for routine volume balance analyses. If the characteristics of the problem are such that the potential for large volume balance errors is large, then the volumes derived with the procedures presented in this paper need to be compared with the volumes computed with an unsteady simulation model. Simulation model results can then be used to adjust the β values used in the volume balance calculations. A procedure for carrying out those adjustments is described in a companion paper (Bautista et al. 2012). That procedure can also be used to adjust the shape factor for the infiltrated profile, which is another source of error in volume balance analyses.

The previously discussed analysis focuses on the differences between zero-inertia and volume balance calculations. It should be clear that erroneous determinations of pertinent inputs will lead to larger volume balance errors than shown in this paper. In practical applications of the previously noted procedures, a particular

Table 10. Inputs and Calculations for Practical Example

t min	x_A m	x_{PA} m	V_{in} cum	Q_{in} l/s	V_{ro} m^3	β	y_0 cm	A_0 m^2 (E-02)	σ_y	Pred. V_y m^3	Meas. V_y m^3	E_{VB} (%)
	0.00											
9	30.5		0.84	1.56	0.00	0.40	7.07	1.84	0.60	0.34	0.17	20.1%
20	61.0		1.85	1.51	0.00	0.40	7.72	2.15	0.60	0.78	0.71	3.8%
35	91.4		3.20	1.51	0.00	0.40	8.14	2.36	0.59	1.28	1.11	5.4%
55	121.9		4.98	1.45	0.00	0.40	8.31	2.45	0.59	1.77	1.87	2.0%
77	152.4		6.90	1.45	0.00	0.40	8.52	2.55	0.59	2.31	2.48	2.5%
91	168.6		8.11	1.43	0.00	0.40	8.55	2.57	0.59	2.57	2.79	2.7%
100	168.6	179.0	8.89	1.44	0.09	0.40	8.62	2.61	0.62	2.74	2.88	1.5%
120	168.6	201.2	10.63	1.43	0.54	0.40	8.70	2.65	0.67	3.00	3.06	0.6%
149	168.6	231.1	13.03	1.34	1.40	0.40	8.60	2.60	0.72	3.15	3.17	0.2%
180	168.6	260.8	15.54	1.35	2.33	0.40	8.69	2.65	0.75	3.37	3.24	0.8%
210	168.6	287.9	17.95	1.32	3.23	0.40	8.71	2.66	0.78	3.49	3.22	1.5%
235	168.6	309.4	19.93	1.32	3.98	0.40	8.75	2.68	0.80	3.59	2.96	3.2%

Note: V_{ro} = Runoff volume; Pred = Predicted; Meas = Measured. All other variables as previously defined.

challenge is the determination of the roughness coefficient. Thus, determinations of surface volume need to incorporate sensitivity and/or error analyses to test primarily the effect of the uncertain roughness.

Previous studies (Esfandiari and Maheshwari 1997) have shown that large field undulations relative to the average slope cause substantial variation in the depth profile. Such conditions may complicate or altogether invalidate the application.

Conclusions

In surface irrigation volume balance analyses, upstream flow depth and the surface shape factor can be calculated by assuming that the surface depth profile varies as a power law. Such an approach requires prior knowledge of the exponent of that power law, β. The variation of β as a function of advance distance and system properties was examined using a system of dimensionless variables using unsteady flow simulation. β varies over a narrow range and, thus, can be assumed constant with advance distance in practical volume balance calculations, when the field bottom slope is small, infiltration rates vary widely as a function of opportunity time, and the field length is short relative to the maximum distance that water can advance with the given flow. In contrast, β varies widely with advance distance when the slope is steep, when infiltration rates are relatively constant during the event, and with long fields (relative to the maximum advance distance). Estimating β as a function of advance distance is most challenging under these latter conditions.

Practical relationships for β as a function of field slope only are proposed. These relationships will result in reasonable estimates for the flow depth, but not necessarily for the surface shape factor. Because surface storage as a fraction of the applied volume decreases with increasing advance distance, these errors may have a small effect on the accuracy of volume balance calculations. This is particularly true with large field slopes. Very large volume balance errors are possible with large field slopes, however, if the distance advanced by the water is small and if the infiltration rate is a relatively constant term and the field length is close to the maximum distance that water can advance with the given flow. In those cases, the infiltrated volume grows slowly relative to the applied volume. Users of volume balance procedures need to be aware of conditions in which these systematic errors are large and more sophisticated determinations of β are needed.

Notation

The following symbols are used in this paper:

a = empirical infiltration exponent;
A_0 = upstream flow sectional area;
b, B = empirical infiltration steady-infiltration rate constant;
B^* = dimensionless furrow irrigation parameter;
BW = bottom width for a trapezoidal furrow;
c = constant of the power law relationship for top width as a function of flow depth;
D_0^* = dimensionless furrow irrigation parameter;
FS = furrow spacing;
k, K = empirical infiltration constant;
K^* = dimensionless furrow irrigation parameter;
L_f = field length;
m = exponent of the power law relationship for top width as a function of flow depth;
n = Manning roughness coefficient;
Q_0 = inflow rate;
R = hydraulic radius;
S_f = friction gradient;
SS = side slope for a trapezoidal furrow;
S_0 = field bottom slope;
T = top width;
t = time;
t_{co} = cutoff time;
t_{req} = time required to infiltrate the required infiltration depth z_{req};
t_x = advance time to distance x;
V_{in} = inflow volume;
V_y = surface storage volume;
V_Z = infiltration volume;
x = distance along stream;
x_A = advance distance;
y = flow depth;
y_n = normal flow depth;
y_0 = upstream flow depth;
Z = infiltration volume per unit length;

z = infiltration volume per unit area;
z_{req} = required infiltration depth;
β = exponent of the power law relationship for y(x);
λ = relative contribution of the steady-state infiltrati; on term to z_{req} in t_{req}; and
σ_y = surface shape factor.

References

Bautista, E., Clemmens, A. J., Strelkoff, T. S., and Schlegel, J. (2009). "Modern analysis of surface irrigation systems with WinSRFR." *Agric. Water Manage.*, 96, 1146–1154.

Bautista, E., Strelkoff, T. S., and Clemmens, A. J. (2012). "Errors in infiltration calculations in volume-balance models." *J. Irrig. Drain. Eng.*, 138(8), 727–735.

Bautista, E., Strelkoff, T. S., Clemmens, A. J., and Zerihun, D. (2008). "Surface volume estimates for infiltration parameter estimation." *Proc. World Environmental and Water Resources Congress 2008 – Ahupua'A*, R. W. Babcok, and R. Walton, eds., ASCE/Environmental and Water Resources Institute (EWRI), CDROM.

Esfandiari, M., and Maheshwari, B. L. (1997). "Field values of the shape factor for estimating surface storage in furrows on a clay soil." *Irrig. Sci.*, 17(4), 157–161.

Gillies, M. H., and Smith, R. J. (2005). "Infiltration parameters from surface irrigation advance and runoff data." *Irrig. Sci.*, 24(1), 25–35.

Katopodes, N. D., and Strelkoff, T. S. (1977). "Dimensionless solutions of border irrigation advance." *J. Irrig. and Drain. Div.*, 103(4), 401–417.

Monserrat, J., and Barragan, J. (1998). "Estimation of the surface volume in hydrological models for border irrigation." *J. Irrig. Drain. Eng.*, 124(5), 238–247.

Perea, H. (2005). "Development, verification, and evaluation of a solute transport model in surface irrigation." PhD. dissertation, Agricultural and Biosystems Engineering Dept., Univ. of Arizona, Tucson.

Scaloppi, E. J., Merkley, G. P., and Willardson, L. S. (1995). "Intake parameters from advance and wetting phases of surface irrigation." *J. Irrig. Drain. Eng.*, 121(1), 57–70.

Strelkoff, T. S. (1985). "Dimensionless formulation of furrow irrigation." *J. Irrig. Drain. Eng.*, 111(4), 380–394.

Strelkoff, T. S., and Clemmens, A. J. (1994). "Dimensional analysis in surface irrigation." *Irrig. Sci.*, 15(2-3), 57–82.

Strelkoff, T. S., and Clemmens, A. J. (2007). "Hydraulics of surface systems." Chapter 13, *Design and operation of farm irrigation systems*, G. Hoffman, R. G. Evans, M. E. Jensen, D. L. Martin, and R. L. Elliott, eds., 2nd Ed., American Society of Agricultural and Biological Engineers, St. Joseph, MI, 437–498.

Strelkoff, T. S., Clemmens, A. J., El-Ansary, M., and Awad, M. (1999). "Surface-irrigation evaluation models: Application to level basins in Egypt." *Trans. ASAE*, 42(4), 1027–1036.

Valiantzas, J. D. (1993). "Border advance using improved volume-balance model." *J. Irrig. Drain. Eng.*, 119(6), 1006–1025.

Valiantzas, J. D. (1997). "Volume balance irrigation advance equation: Variation of surface shape factor." *J. Irrig. Drain. Eng.*, 123(4), 307–312.